



## Nitrogen removal of the simultaneous anammox and denitrification process for treating phenol-containing sewage in a hybrid UASB reactor

Zhaozhao Wang<sup>a,b</sup>, Ying Ji<sup>a,b</sup>, Lina Yan<sup>c</sup>, Dan Zhao<sup>a,b</sup>, Simin Li<sup>a,b,\*</sup>

<sup>a</sup>College of Energy and Environmental Engineering, Hebei University of Engineering, Handan 056038, China, Tel. +8617831917609; emails: 18303233729@163.com (S. Li), W-Z-Z@163.com (Z. Wang), 18244606382@139.com (Y. Ji), 18732059211@163.com (D. Zhao)

<sup>b</sup>Center for Water Pollution Control and Water Ecological Remediation, Hebei University of Engineering, Handan 056038, China

<sup>c</sup>Graduate Department of Hebei University of Engineering, Handan 056038, China, email: yanlina01@126.com (L. Yan)

Received 3 May 2018; Accepted 27 November 2018

### ABSTRACT

A simultaneous anammox and denitrification (SAD) process was applied for removing organic and nitrogen contaminants in an upflow anaerobic sludge blanket (UASB) reactor treating phenol-containing sewage. The morphologies of the granular sludges were further investigated. The results demonstrated that the SAD process could be successfully started up after a continuous operation for 86 d when the hydraulic retention time was maintained at 1.5 h. The removal efficiencies of ammonia, nitrite, and total nitrogen were 85.4%, 86.1%, and 79.9%, respectively. A suppressed anammox bacterial (AMX) activity and a decreased contribution ratio of the nitrogen removal via anammox pathway were observed and resulted from the increased chemical oxygen demand (COD)/NO<sub>x</sub>-N (COD/N) ratio ( $\geq 0.34$ ). Batch substrate degradation tests verified the stable activity of the AMX and denitrification bacteria (DNB) after long-term operation of the optimized SAD process (COD/N ratio of 0.32). Three kinds of granular sludges (anammox, denitrification, and SAD granular sludges) formed at the bottom of the hybrid UASB reactor and originated from the sole anammox granular sludge at the inoculation stage. Photos and scanning electron microscopy images of the SAD granular sludge illustrated the coexistence of the AMX (red, spherical, inner part of the granular sludge) and the DNB (white, short rod, outer part of the granular sludge). Furthermore, the average particle size of the granular sludges increased and the major fraction shifted from 0–1.5 mm (69.4%) to 0.5–2.0 mm (68.9%), indicating the granulation of the sludge mixture by coupling the heterotrophic denitrification process.

*Keywords:* Nitrogen removal; Anammox; Denitrification; COD/N ratio; Granular sludge characterization

### 1. Introduction

The eutrophication of a water body resulting from the increased nitrogen discharge is one of the main factors leading to the deterioration of the water environment, which has drawn global attention in environmental research [1,2]. A variety of biological treatment processes based on the theory of nitrification and denitrification have been developed to remove nitrogen from sewage efficiently [3–5].

Different from conventional biological nitrogen removal processes, the anammox process is achieved by a class of autotrophic bacteria belonging to the phylum *Planctomycetes*,

which can directly oxidize ammonium under anoxic conditions using nitrite as a terminal electron acceptor. This process has been verified as a more efficient and economically viable method for nitrogen removal [6]. However, the nitrogen removal performance cannot be further improved due to the nitrate production during this process. In addition, the anammox bacteria (AMX) are susceptible to unfavorable existing environmental factors such as toxic organic compounds (e.g., phenol), showing an inhibiting effect. Nitrogen and phenolic compounds regularly exist in certain industrial sewage, such as coke-oven sewage [7], resin-producing sewage [8], and petrochemical sewage [9], and pose a severe

\* Corresponding author.

challenge to the anammox process for nitrogen removal when toxic organic compounds are present.

Recent study findings have shown that the coupling of the anammox and denitrification processes can be achieved by the coexistence of AMX and denitrification bacteria (DNB) for advanced nitrogen removal [10,11]. Qiao et al. [12] reported that electrochemical technology could be employed as an enhanced tool for integrating the anammox and the autotrophic denitrification processes. While Ge et al. [13] found that the DNB could be easily cultivated under the driven station of organic matter and powder activated carbon.

The DNB can utilize the organic compounds as electron donors to denitrify the nitrate that is produced during the anammox process, which reduces the suppression of the activity of the AMX. Influent organic carbon was proved to be critical for the stable operation of the simultaneous anammox and denitrification (SAD) processes [14]. At low chemical oxygen demand (COD)/N ratios, electron donors for nitrogen removal could be obtained from both ammonium and organic compounds [15]. He et al. found that AMX and DNB had a better synergistic effect for efficient nitrogen removal at COD/N ratio of 0.53 [16].

When the influent COD/N ratios increase beyond a certain level, the DNB can outcompete the AMX for the nitrite (electron acceptors) due to the decreased AMX activity. In the anammox-denitrification system, the higher COD/N ratio that resulted from the increased concentration of organic matter induced the deterioration of the nitrogen removal efficacy [17]. Furthermore, the increasingly strong denitrification process will cause a weakening of the coupling efficiency of the SAD process [18]. Conversely, nitrite accumulation from partial denitrification promotes anammox behaviors for lower COD/N ratios [17]. Cervantes et al. [19] revealed that the carbon source played an important role for ammonium and nitrate removal because ammonium is oxidized in the anammox process by nitrite through dissimilatory nitrate reduction.

Thus, the influent carbon source plays an important role in regulating the synergy of the anammox and denitrification processes in the SAD process [20]. The impacts of phenol on the anammox process are significantly different from those of readily degradable organic compounds. It has been found that the AMX activity is clearly inhibited under phenol stress, whereas it can be recovered without phenol addition for which a lag period is required [21]. The anammox process can be applied to nitrogen-containing phenolic sewage if the inhibition of the AMX activity induced by the phenol can be reduced. Ramos et al. [22] reported that phenol could be utilized by DNB as the sole organic carbon source in an anoxic granular reactor. González-Blanco et al. [23,24] discovered that ammonium and *p*-cresol could supply electron donors for nitrite reduction by denitrifying sludge.

Therefore, the SAD process is proposed to enhance the nitrogen removal using phenol as the electron donor for the denitrification pathway, which also reduces the inhibition of the AMX activity during the treatment of nitrogen-containing phenolic sewage.

To date, limited research has been reported on the SAD process using phenol as the sole carbon source. In this study, an upflow anaerobic sludge blanket (UASB) reactor was used to establish the SAD process for the treatment of

phenol-containing sewage. The main objectives of this study were (I) to investigate the start-up characteristics of the SAD process, (II) to establish an optimization strategy for the SAD process, and (III) to investigate the granular sludge variations and long-term stability of the SAD system. These findings will serve as a reference for the optimization and effective practical application of the SAD process in the treatment of phenol-containing sewage.

## 2. Materials and methods

### 2.1. Experimental setup and operational conditions

#### 2.1.1. Continuous-flow experiment

The schematic diagram of the continuous-flow hybrid UASB reactor is depicted in Fig. 1(a). The effective volume was 10 L with a height of 110 cm and an inner diameter of 11 cm. One-third of the reactor was filled with spherical polyvinyl chloride carriers (diameter of 10 cm) and a fibrous annular braided belt to reduce sludge loss. The reactor was wrapped with black soft materials to reduce the light, and a circulating water bath system was used to maintain the temperature (~25°C). The synthetic sewage with a controlled pH value (~7.8) was pumped to the bottom of the reactor using a peristaltic pump, and a hydraulic retention time (HRT) of 1.5 h was maintained. The operational strategy of the hybrid UASB reactor was divided into three stages, including the start-up phase (phase I–IV), optimization phase (phase V–VIII), and long-term operation phase (phase IX) of the SAD process, as shown in Table 1. During the start-up stage, the phenol was added stepwise (from 0 to 18.8 mg L<sup>-1</sup>, with a COD/NO<sub>x</sub>-N (COD/N) ratio of 0–0.34) to the continuous-flow system. Thereafter, the SAD process was expected to be optimized by regulating the phenol concentrations with the COD/N ratios in the range of 0.31–0.62. Finally, the SAD process was operated for a prolonged period of 60 d.

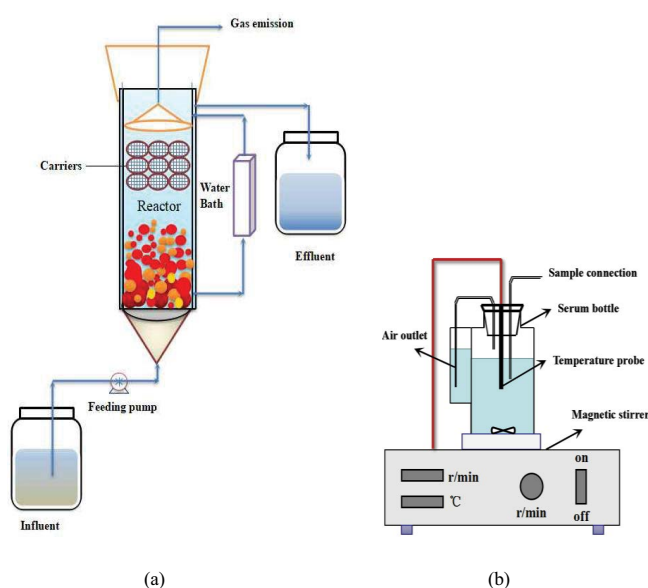


Fig. 1. Schematic diagram of the reactors (a) UASB reactor and (b) sequencing batch reactor.

Table 1  
Substrate concentrations in the feed of the hybrid UASB reactor

Phases	Operation strategy	Periods (d)	NH <sub>4</sub> <sup>+</sup> -N (mg L <sup>-1</sup> )	NO <sub>2</sub> <sup>-</sup> -N (mg L <sup>-1</sup> )	NO <sub>3</sub> <sup>-</sup> -N (mg L <sup>-1</sup> )	Phenol (mg L <sup>-1</sup> )	COD/N ratio
Start-up of the SAD process							
I		1–6	100.5	106.0	6.6	0	0
II		7–14	98.2	107.1	6.0	9.4	0.16
III		15–35	93.7	98.5	4.7	9.4	0.17
		36–58	107.7	97.1	4.8	14.1	0.24
		59–80	90.0	96.0	5.8	18.8	0.31
IV		81–86	70.7	88.9	4.6	18.8	0.34
Optimization of the SAD process							
V		87–98	77.2	88.4	8.6	28.2	0.62
VI		99–105	79.6	91.8	8.0	37.6	0.78
VII		106–110	76.7	93.1	8.9	56.4	1.18
VIII		111–120	74.3	94.9	10.6	18.8	0.30
IX	Long-term operation of the SAD process	121–180	60.8	90.5	9.9	18.8	0.32

Note: The average values of the experimental data are presented in the table.

### 2.1.2. Sequencing batch tests

A 500-mL serum bottle was used to demonstrate the sequencing batch tests, as shown in Fig. 1(b). First, the mixed granular sludges were collected from the hybrid UASB reactor and washed using deionized water for removal of the residue. Then, the serum bottle, to which 150 mL sludge and 350 mL of a prepared matrix were added, was placed on a magnetic stirrer (500 rpm) with high-purity nitrogen blown in to remove the dissolved oxygen (DO) when the activity tests of the anammox and denitrification were performed. The control temperature was maintained at 25°C ± 1°C. The pH values were measured before and after the sequencing batch tests.

## 2.2. Characteristics of synthetic phenol-containing sewage and inoculation sludge

### 2.2.1. Synthetic phenol-containing sewage

The synthetic sewage was composed of NH<sub>4</sub>Cl, NaNO<sub>2</sub>, and phenol as the main sources of ammonium, nitrite, and organic carbon, respectively. The concentrations of ammonium, nitrite, and organic carbon were regulated according to the requirements of the experiment. The other components included NaHCO<sub>3</sub> (800–1,000 mg L<sup>-1</sup>), KH<sub>2</sub>PO<sub>4</sub> (25 mg L<sup>-1</sup>), MgSO<sub>4</sub>·7H<sub>2</sub>O (480 mg L<sup>-1</sup>), CaCl<sub>2</sub>·2H<sub>2</sub>O (180 mg L<sup>-1</sup>), trace element solution I (1 mg L<sup>-1</sup>), and trace element solution II (1 mg L<sup>-1</sup>). The trace element solution I contained ethylene diamine tetraacetic acid (EDTA) (5,000 mg L<sup>-1</sup>) and FeSO<sub>4</sub>·7H<sub>2</sub>O (5,000 mg L<sup>-1</sup>). The trace element solution II contained EDTA (15,000 mg L<sup>-1</sup>), ZnSO<sub>4</sub>·7H<sub>2</sub>O (430 mg L<sup>-1</sup>), CoCl<sub>2</sub>·6H<sub>2</sub>O (240 mg L<sup>-1</sup>), MnCl<sub>2</sub>·4H<sub>2</sub>O (990 mg L<sup>-1</sup>), CuSO<sub>4</sub>·5H<sub>2</sub>O (250 mg L<sup>-1</sup>), Na<sub>2</sub>MoO<sub>4</sub>·2H<sub>2</sub>O (220 mg L<sup>-1</sup>), NiCl<sub>2</sub>·6H<sub>2</sub>O (190 mg L<sup>-1</sup>), Na<sub>2</sub>SeO<sub>4</sub>·10H<sub>2</sub>O (210 mg L<sup>-1</sup>), and H<sub>3</sub>BO<sub>3</sub> (14 mg L<sup>-1</sup>). The specific synthetic sewage qualities were as follows: NH<sub>4</sub><sup>+</sup>-N, 44.2–133.2 mg L<sup>-1</sup>; NO<sub>2</sub><sup>-</sup>-N,

63.9–131.2 mg L<sup>-1</sup>; NO<sub>3</sub><sup>-</sup>-N, 1.3–13.4 mg L<sup>-1</sup>; phenol, 0–56.4 mg L<sup>-1</sup>; pH, 7.6–8.0.

### 2.2.2. Inoculation sludge

The inoculation anammox granular sludge was collected from a 50-L UASB reactor that had been operated in a stable manner for about 2 years. The main species of AMX present in the reactor was *Candidatus Brocadia fulgida* (JX852965–JX852969). The inoculation sludge was injected into the hybrid UASB reactor, resulting in a mixed liquor volatile suspended solid (MLVSS) concentration of 5,000 mg L<sup>-1</sup>.

## 2.3. Chemical analysis and calculation procedures

NH<sub>4</sub><sup>+</sup>-N, NO<sub>2</sub><sup>-</sup>-N, NO<sub>3</sub><sup>-</sup>-N, the mixed liquor suspended solids (MLSS), and the MLVSS were analyzed according to standard methods [25]. Phenol was measured by high-performance liquid chromatography (HPLC) [22] using an UltiMate 3000 (Dionex Corporation, USA) with an Agilent Zorbax SB-C18, USA (4.6 mm × 100 mm × 3.5 μm) column and a UV detector set at 254 nm; the flow rate was 1.875 mL min<sup>-1</sup>, and the column temperature was maintained at 30°C. The mobile phases were acidified water (ultrapure water containing H<sub>2</sub>SO<sub>4</sub> at pH 1.41) and HPLC-grade methanol following a gradient elution. The gradient started from 100% of acidified water and progressively changed to 50:50 v/v of water: methanol in 18 min and then it remained isocratic until 20 min. The injection volume was 20 μL, and the maximum pressure in the column was approximately 290,000 hPa.

The DO, pH, and temperatures were determined by a multiparameter sensor (WTW Multi 3420i, Germany). The morphological characteristics of the granular sludge specimens were observed using a scanning electron microscopy (SEM) (S-4300, Hitachi, Japan). The particle sizes of

the granular sludges were determined using standard test screens (GB6003.1-1997).

The consumptions of  $\text{NH}_4^+\text{-N}$  and  $\text{NO}_2^-\text{-N}$ , the production of  $\text{NO}_3^-\text{-N}$ , the removal efficiencies of  $\text{NH}_4^+\text{-N}$ ,  $\text{NO}_2^-\text{-N}$ , and the total nitrogen (TN), the nitrogen loading rate (NLR), ( $\text{kg m}^{-3} \text{d}^{-1}$ ), and the nitrogen removal rate (NRR) ( $\text{kg m}^{-3} \text{d}^{-1}$ ) were calculated according to the following equations:

$$\text{NH}_4^+\text{-N consumption} = \Delta\text{NH}_4^+\text{-N} = \text{NH}_4^+\text{-N}_{\text{inf}} - \text{NH}_4^+\text{-N}_{\text{eff}} \quad (1)$$

$$\text{Removal efficiency of NH}_4^+\text{-N} = \frac{\text{NH}_4^+\text{-N}_{\text{inf}} - \text{NH}_4^+\text{-N}_{\text{eff}}}{\text{NH}_4^+\text{-N}_{\text{inf}}} \times 100\% \quad (2)$$

$$\text{NO}_2^-\text{-N consumption} = \Delta\text{NO}_2^-\text{-N} = \text{NO}_2^-\text{-N}_{\text{inf}} - \text{NO}_2^-\text{-N}_{\text{eff}} \quad (3)$$

$$\text{Removal efficiency of NO}_2^-\text{-N} = \frac{\text{NO}_2^-\text{-N}_{\text{inf}} - \text{NO}_2^-\text{-N}_{\text{eff}}}{\text{NO}_2^-\text{-N}_{\text{inf}}} \times 100\% \quad (4)$$

$$\text{NO}_3^-\text{-N production} = \Delta\text{NO}_3^-\text{-N} = \text{NO}_3^-\text{-N}_{\text{eff}} - \text{NO}_3^-\text{-N}_{\text{inf}} \quad (5)$$

$$\text{Removal efficiency of TN} = \frac{\text{TN}_{\text{inf}} - \text{TN}_{\text{eff}}}{\text{TN}_{\text{inf}}} \times 100\% \quad (6)$$

$$\text{NLR} = \text{NH}_4^+\text{-N} = \frac{\text{TN}_{\text{inf}}}{\text{HRT}} \quad (7)$$

$$\text{NRR} = \text{NH}_4^+\text{-N} = \frac{\text{TN}_{\text{inf}} - \text{TN}_{\text{eff}}}{\text{HRT}} \quad (8)$$

where  $\text{NH}_4^+\text{-N}_{\text{inf}}$ ,  $\text{NO}_2^-\text{-N}_{\text{inf}}$ ,  $\text{NO}_3^-\text{-N}_{\text{inf}}$  and  $\text{TN}_{\text{inf}}$  are the influent concentrations of  $\text{NH}_4^+\text{-N}$ ,  $\text{NO}_2^-\text{-N}$ ,  $\text{NO}_3^-\text{-N}$ , and TN ( $\text{mg L}^{-1}$ ), respectively, and  $\text{NH}_4^+\text{-N}_{\text{eff}}$ ,  $\text{NO}_2^-\text{-N}_{\text{eff}}$ ,  $\text{NO}_3^-\text{-N}_{\text{eff}}$  and  $\text{TN}_{\text{eff}}$  are the effluent concentrations of  $\text{NH}_4^+\text{-N}$ ,  $\text{NO}_2^-\text{-N}$ ,  $\text{NO}_3^-\text{-N}$ , and TN ( $\text{mg L}^{-1}$ ), respectively. HRT is the hydraulic retention time (d).

### 3. Results and discussion

#### 3.1. The start-up of the SAD process

The start-up period of the SAD process was divided into four suboperational phases (as shown in Fig. 2) according to the phenol dosage and nitrogen removal performance. In phase I (Days 1–6, without phenol dosage), the average removal efficiencies of  $\text{NH}_4^+\text{-N}$ ,  $\text{NO}_2^-\text{-N}$ , and TN increased from 16.2%, 16.8%, and 14.3% to 25.4%, 24.9%, and 21.9%, respectively. Furthermore, the  $\text{NO}_3^-\text{-N}$  concentration was higher in the effluent than in the influent, indicating that the AMX activity was gradually enhanced, and the inoculated anammox granular sludge was able to adapt to the new cultivation environment. On Day 7 of the phase II (Days 7–14, AMX adaptation phase with COD/N ratio of 0.16), a sharp 10% reduction in the removal efficiency was observed for  $\text{NH}_4^+\text{-N}$ ,  $\text{NO}_2^-\text{-N}$ , and TN. This indicated that the phenol addition had a negative impact on the anammox process

and the AMX activity deteriorated in the presence of toxic organic matter [21,26]. However, the average removal efficiencies of  $\text{NH}_4^+\text{-N}$ ,  $\text{NO}_2^-\text{-N}$ , and TN gradually recovered to the previous levels after the 7 d operation, affirming that the anammox granular sludge was capable of tolerating a shock with a low concentration of toxic organic matter ( $9.4 \text{ mg L}^{-1}$ ) and that the AMX could exhibit activity for the phenol-containing treatment. The average phenol concentration in the effluent was  $7.5 \text{ mg L}^{-1}$  with an average removal efficiency of 20% through phase II.

In phase III (Days 15–80, AMX activity improvement phase), the phenol concentration was increased stepwise from 9.4 to  $18.8 \text{ mg L}^{-1}$  (COD/N ratio of 0.17–0.31), in order to achieve a fast start-up of the SAD process due to the enrichment of the AMX and the increased  $\text{NO}_3^-\text{-N}$  production for the electron donors. The average influent concentrations of  $\text{NH}_4^+\text{-N}$  and  $\text{NO}_2^-\text{-N}$  were maintained at 97.1 and  $97.2 \text{ mg L}^{-1}$ , respectively, throughout this phase. Nevertheless, the average effluent concentrations of  $\text{NH}_4^+\text{-N}$  and  $\text{NO}_2^-\text{-N}$  decreased to 7.7 and  $10.5 \text{ mg L}^{-1}$ , respectively, and the corresponding removal efficiencies were 89.6% and 87.9%, respectively. The average removal efficiency of the phenol increased from 42.8% to 69.4%, suggesting that more carbon sources were employed as electron donors.

The increase in the  $\text{NH}_4^+\text{-N}$  and  $\text{NO}_2^-\text{-N}$  removals demonstrated the enhancement of the AMX activity. In addition, the ratio of  $\text{NO}_3^-\text{-N}$  production to  $\text{NH}_4^+\text{-N}$  consumption was found to be lower than the theoretical stoichiometric value (0.26) [27], proving that the phenol was used as an electron donor by the DNB. Overall, the TN removal efficiency was significantly improved from 22.1% to 83.7% as a result of the coexistence of the AMX and DNB in the SAD process in spite

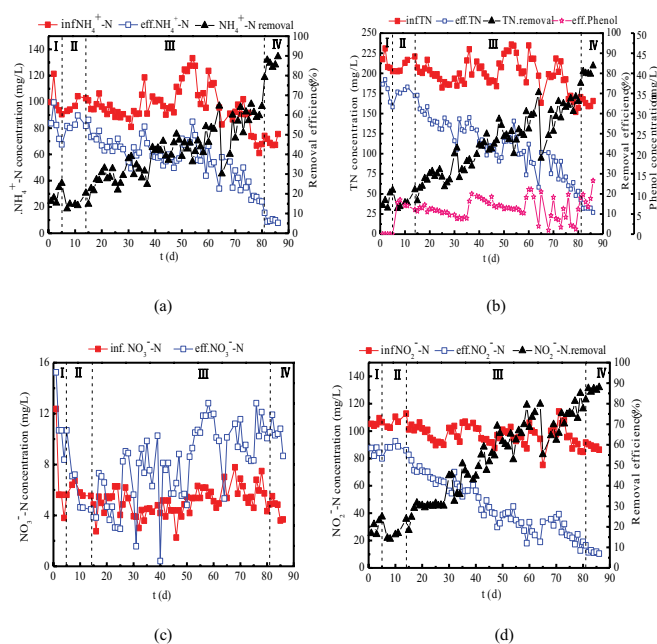


Fig. 2. Nitrogen removal performance in the UASB reactor during the start-up period. (a) Ammonia concentrations and removal and (b) TN concentrations and removal; phenol concentrations, (c) nitrate concentrations, and (d) nitrite concentrations and removal.

of a substantial fluctuation of the  $\text{NO}_3^-$ -N concentrations. After phase III, the system came into a short-term stable operation phase (phase IV, Days 81–86, COD/N ratio of 0.34). During this phase, 85.39% of  $\text{NH}_4^+$ -N and 86.12% of  $\text{NO}_2^-$ -N were removed on average and the corresponding effluent concentrations were 10.3 and 12.4  $\text{mg L}^{-1}$ , respectively.

The  $\text{NO}_3^-$ -N production value was 5.9  $\text{mg L}^{-1}$ , resulting in a ratio of  $\text{NO}_3^-$ -N production to  $\text{NH}_4^+$ -N consumption of 0.10. A 50% reduction in the phenol concentration was finally achieved in this phase. These results indicated that the nitrogen removal was achieved by the coupling of the anammox and denitrification processes. Furthermore, 79.9% of TN was removed in this system and the NLR and NRR reached 2.63 and 2.10  $\text{kg m}^{-3} \text{d}^{-1}$ , respectively, suggesting that the SAD process started up successfully.

### 3.2. The optimization of the phenol addition in the SAD process

Fig. 3 shows the nitrogen removal performance of the SAD process in the hybrid UASB reactor during the optimization period. From phase V to VII (Days 87–110), the phenol dosage was increased from 28.2 to 56.4  $\text{mg L}^{-1}$  (COD/N ratio of 0.62–1.18) to investigate the influence of the COD/N ratios on the SAD performance. In phase VIII (Days 111–120), the phenol dosage was decreased to 18.8  $\text{mg L}^{-1}$  (COD/N ratio of 0.30) to study the recovery capability of the SAD process from the high phenol stress. It was observed that the removal efficiencies of  $\text{NH}_4^+$ -N and TN increased rapidly to 29.8% and 52.9% from Day 87 to Day 92 as the COD/N ratio increased from 0.34 to 0.62 in phase V. Meanwhile, the ratio of  $\text{NO}_2^-$ -N consumption to  $\text{NH}_4^+$ -N consumption increased to 3.05 and the ratio of  $\text{NO}_3^-$ -N production to  $\text{NH}_4^+$ -N consumption decreased to  $-0.07$ . This indicated that a high dosage of phenol resulted in a significant inhibition of the AMX activity

but had almost no impacts on the DNB activity. Thereafter, the AMX activity gradually recovered after 6 d operation. Finally, 47.8% of  $\text{NH}_4^+$ -N and 84.9% of  $\text{NO}_2^-$ -N were removed from the system, and the corresponding average concentrations in the effluent were 39.8 and 13.3  $\text{mg L}^{-1}$ , respectively. A short-term stable SAD process was achieved, and the ratio of  $\text{NH}_4^+$ -N consumption to  $\text{NO}_2^-$ -N consumption to  $\text{NO}_3^-$ -N production was 1.00:2.00:0.07.

When the COD/N ratio increased to 0.78 in phase VI, the average effluent concentrations of  $\text{NH}_4^+$ -N and  $\text{NO}_2^-$ -N were 41.5 and 11.9  $\text{mg L}^{-1}$ , respectively. In phase VII, the average effluent concentrations of  $\text{NH}_4^+$ -N and  $\text{NO}_2^-$ -N decreased to 37.1 and 3.3  $\text{mg L}^{-1}$ , respectively, as the COD/N ratio reached 1.18. Meanwhile, the ratio of  $\text{NO}_2^-$ -N consumption to  $\text{NH}_4^+$ -N consumption increased from 2.09 in phase VI to 2.28 in phase VII, and the ratio of  $\text{NO}_3^-$ -N production to  $\text{NH}_4^+$ -N consumption decreased from  $-0.04$  in phase VI to  $-0.13$  in phase VII. It was observed that the ratio of  $\text{NO}_2^-$ -N consumption to  $\text{NH}_4^+$ -N consumption increased with the increase in the COD/N ratios, and the ratio values were higher than the theoretical value of 1.32. Conversely, the ratio of  $\text{NO}_3^-$ -N production to  $\text{NH}_4^+$ -N consumption decreased with the increasing COD/N ratios, and the ratios were lower than the theoretical value of 0.26. This suggested that the denitrification process was enhanced at higher COD/N ratios, which exerted an adverse influence on the anammox process in the coupled system. The average consumption values and percentages of the anammox and denitrification routes for the nitrogen removal were further calculated according to the nitrogen mass balance, as illustrated in Table 2. The nitrate and nitrite reductions through denitrification were further estimated through phenol biodegradation. The amounts of denitrified nitrate and nitrite and biodegraded phenol were in accordance with the stoichiometric ratios of Eqs. 9 and 10 [28].

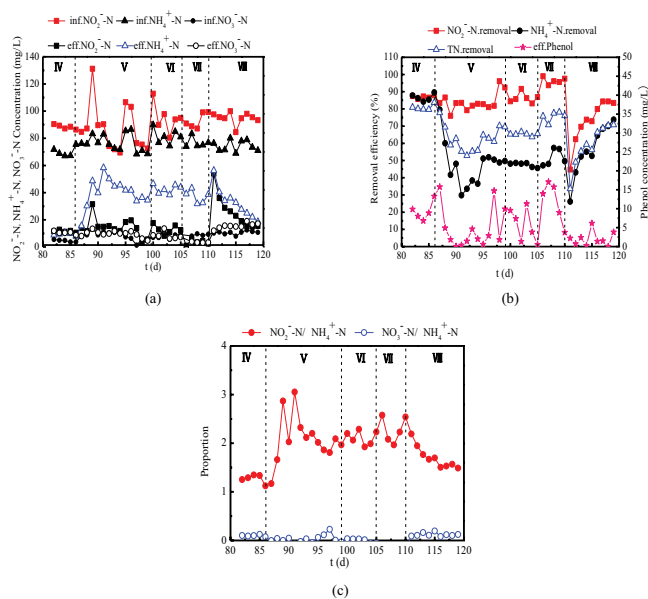
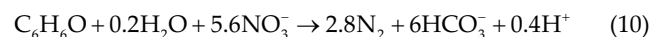
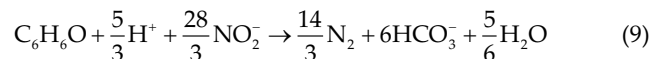


Fig. 3. Nitrogen removal performance in the UASB reactor during the optimization period. (a)  $\text{NO}_2^-$ -N,  $\text{NH}_4^+$ -N, and  $\text{NO}_3^-$ -N concentrations, (b)  $\text{NO}_2^-$ -N,  $\text{NH}_4^+$ -N, and TN removals and phenol concentration, and (c) stoichiometric ratios.



It can be seen that the average nitrogen removal percentage was 85.3% for the anammox route but only 14.7% for the denitrification route, indicating the dominant role of the anammox process in the nitrogen removal in phase IV (COD/N ratio of 0.34). However, the competition increased between the AMX and DNB for electron acceptors ( $\text{NO}_2^-$ -N) as the COD/N ratio increased. Furthermore, the denitrification process was gradually strengthened and resulted from the higher growth rate of the DNB and the inhibition of the AMX activity at a higher COD/N ratio. The average nitrogen removal percentage for the denitrification route increased to 38.4%, while the anammox contribution decreased to 61.6% in phase VII (COD/N ratio of 1.18). It was expected that the anammox route would play a dominant role in the nitrogen removal in the SAD process for the stable operation of the coupled system. The dominant nitrogen removal processes shifted from the anammox process to the denitrification process due to competition for living space under high organic substrate conditions during long-term

Table 2  
Average consumption and percentages of different routes for the nitrogen removal

Consumption	Removal route	IV	V	VI	VII
NH <sub>4</sub> <sup>+</sup> -N removed (mg L <sup>-1</sup> )	Anammox	52.0	39.5	38.0	39.7
NO <sub>2</sub> <sup>-</sup> -N removed (mg L <sup>-1</sup> )	Anammox	68.7	52.1	50.2	52.3
	Denitrification	10.5	24.6	29.6	37.4
NO <sub>3</sub> <sup>-</sup> -N removed (mg L <sup>-1</sup> )	Denitrification	8.0	6.3	10.0	15.8
TN removed (mg L <sup>-1</sup> )	Anammox	107.2	81.3	78.3	81.7
	Denitrification	18.5	30.9	39.6	53.2
Contribution percentage of nitrogen removal routes (%)	Anammox	85.3	72.8	66.6	61.6
	Denitrification	14.7	27.2	33.4	38.4

operation [29]. Thus, the COD/N ratio was decreased to 0.30 (in phase VIII) in case of the AMX washout. After 10 d operation, the AMX activity was recovered and was followed by the stable operation of the SAD process and the ratio of NH<sub>4</sub><sup>+</sup>-N consumption to NO<sub>2</sub><sup>-</sup>-N consumption to NO<sub>3</sub><sup>-</sup>-N production was 1.00:1.52:0.11.

### 3.3. Nitrogen removal during long-term operation of the SAD process

Fig. 4 shows the nitrogen removal performance of the SAD process at the constant COD/N ratio of 0.32 during the long-term operation phase (phase IX, Days 121–180); 98% of NH<sub>4</sub><sup>+</sup>-N and 97.9% of NO<sub>2</sub><sup>-</sup>-N were removed and the corresponding effluent concentrations were 1.30 and 1.93 mg L<sup>-1</sup>, respectively. Overall, the average removal efficiency of the TN was 87.51% and the NLR and NRR were 2.53 and 2.26 kg m<sup>-3</sup> d<sup>-1</sup>, respectively. Moreover, 87.2% of phenol could be removed with the effluent concentration of 2.41 mg L<sup>-1</sup> on average, indicating the stability of the coupled processes of anammox and denitrification by using phenol as the carbon source.

The average NO<sub>3</sub><sup>-</sup>-N production in this system was 6.98 mg L<sup>-1</sup>, and the obtained stoichiometric ratio of NH<sub>4</sub><sup>+</sup>-N consumption to NO<sub>2</sub><sup>-</sup>-N consumption to NO<sub>3</sub><sup>-</sup>-N production was 1.00:1.49:0.12. The theoretical stoichiometric ratio is 1.00:1.32:0.26; it was speculated that both the NO<sub>3</sub><sup>-</sup>-N (10.02 mg L<sup>-1</sup>) and the NO<sub>2</sub><sup>-</sup>-N (8.48) mg L<sup>-1</sup> served as electron acceptors for the DNB. In spite of the competition for NO<sub>2</sub><sup>-</sup>-N between the DNB and the AMX, most of the nitrogen removal still occurred during the anammox process (contribution of 86.82%) due to the sufficient amount of NO<sub>2</sub><sup>-</sup>-N in the influent, which maintained the long-term stability of the SAD system.

Batch tests of the AMX and DNB activities were performed at the end of the long-term operation. The MLVSS concentration of the batch rig after testing was determined (3,475 mg L<sup>-1</sup>). Moreover, the pH value was higher (8.327) after the test than before the test (7.811) as a result of the hydron consumptions during the anammox and denitrification processes. As illustrated in Fig. 5, good negative linear correlations were obtained for the biodegradation processes of NH<sub>4</sub><sup>+</sup>-N ( $R^2 = 0.996$ ) and NO<sub>2</sub><sup>-</sup>-N ( $R^2 = 0.9801$ ), respectively.

The ratio of the specific degradation rates (SDRs) of NO<sub>2</sub><sup>-</sup>-N (1.21 mg g<sup>-1</sup> h) to NH<sub>4</sub><sup>+</sup>-N (0.85 mg g<sup>-1</sup> h) was 1.42, which was higher than the theoretical ratio of 1.32, further proving the competition between AMX and DNB for NO<sub>2</sub><sup>-</sup>-N. The ratio of SDRs of NO<sub>3</sub><sup>-</sup>-N (0.122 mg g<sup>-1</sup> h) to NH<sub>4</sub><sup>+</sup>-N was 0.14, which was lower than the theoretical ratio of 0.26. It was speculated that NO<sub>3</sub><sup>-</sup>-N was denitrified by the DNB using phenol as electron donor due to the declining trend of the phenol biodegradation. Overall, the test results of the batch rig were in agreement with the results of the continuous-flow test, verifying that nitrogen was removed by the coupled anammox and denitrification processes using phenol as a carbon source.

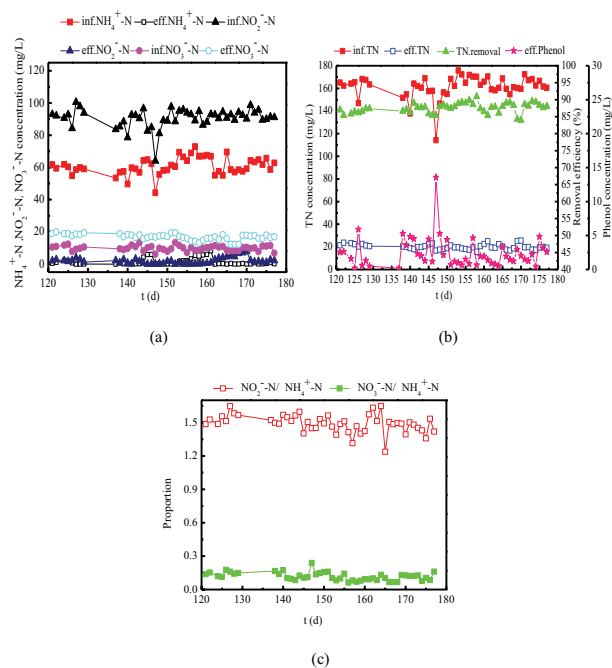


Fig. 4. Nitrogen removal performance in the UASB reactor during long-term operation. (a) NH<sub>4</sub><sup>+</sup>-N, NO<sub>2</sub><sup>-</sup>-N, NO<sub>3</sub><sup>-</sup>-N concentrations, (b) TN concentrations and removal and phenol concentrations, and (c) stoichiometric ratios.

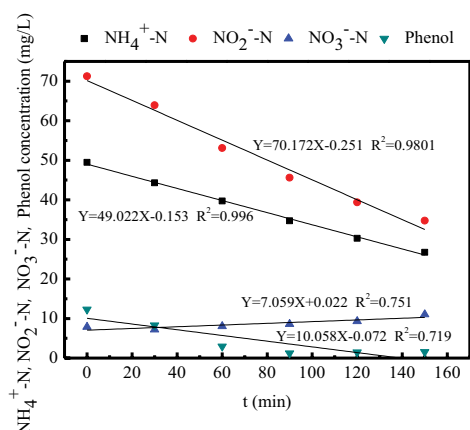


Fig. 5. The activities of the AMX and DNB during long-term operation.

### 3.4. Morphology of granular sludge

#### 3.4.1. Apparent characteristics

Fig. 6 shows the apparent characteristics of the granular sludges at different phases. The average particle size of the inoculated granular sludge was small and the color was brick red as a result of the enriched heme in the AMX cells. Three kinds of granular sludges were formed after the long-term operation of the SAD process (Fig. 6): anammox granular sludge (red) (Fig. 6(a)), phenol-denitrifying granular sludge (white) (Fig. 6(b)), and SAD granular sludge (white, outer part; red, inner part) (Fig. 6(c)). The individual formation of the anammox and phenol-denitrifying granular sludges indicated that sufficient substrates could be obtained by the AMX and DNB from the living environments, respectively. Moreover, it was speculated that the formation of the white sludge (i.e., the independent or the outer part of the anammox granular sludge) indicated that different genera of DNB exhibited different priorities for using  $\text{NO}_2^-$ -N or  $\text{NO}_3^-$ -N as electron acceptors. The formation of the SAD granular sludge further confirmed that the nitrogen removal was achieved by the coupling of the anammox and the denitrification processes. Compared with the phenol-denitrifying granular sludge with irregular shape and a loose structure, the anammox and SAD granular sludges exhibited a regular shape and a dense structure as a result of the self-aggregation of the AMX.

In addition, the broken SAD granular sludge was observed by SEM, as shown in Figs. 7(a) and (b), respectively. Spherical bacteria (referred to AMX) were found in the inner part of the SAD granular sludge and had a diameter of 0.4–0.7  $\mu\text{m}$ , which was slightly smaller than the diameters reported in previous

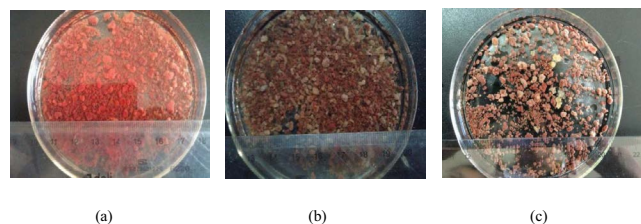


Fig. 6. Photographs of granular sludges. (a) Inoculated granular sludge, (b) granular sludge at the end of phase IX, and (c) broken SAD granular sludge.

studies (0.8–1.1  $\mu\text{m}$ ) [30]. Short-rod bacteria (referred to as DNB) were also discovered in the outer part of the SAD granular sludge, with a size of 0.28–0.37  $\mu\text{m} \times 0.67$ –1.26  $\mu\text{m}$ . These findings further confirmed that the SAD process was achieved by the synergistic effects of two types of bacteria with diverse colors and shapes.

#### 3.4.2. Particle size distribution

The particle size distribution of the granular sludge at the bottom of the hybrid UASB reactor is shown in Table 3. The granular sludge particle size distribution was characterized as the percentage of the MLSS of different particle sizes and the total MLSS. At the inoculation stage (Day 0), 32% of the granular sludge particles were in the range of 0.5–1.0 mm, accounting for the largest proportion. In addition, 19.2%, 17.83%, and 16.22% were in the range of 0–0.5, 1–1.5, and 1.5–2.0 mm, respectively; 14.43% were larger than 2.0 mm in size. There were substantial differences in the granular sludge particle size distribution between the inoculation stage and the end of the operation (Day 180). More specifically, the largest fraction of the granular sludge particles shifted from the range of 0.5–1.0 mm to the range of 1.5–2 mm (30.87%). The proportion of sludge particles in the range of 0–1.0 mm decreased to 22.8%. Nevertheless, a proportional increase of 11.83% was observed for sludge particles of >2 mm size. Thus, the granular sludge particle size increased at the end of the operation. The possible reasons are (1) the enrichment of the AMX and the growth of the anammox granular sludges, (2) the enrichment of the DNB and the formation of denitrifying granular sludge, and (3) the growth of the DNB on the anammox granular sludges and the formation of the SAD granular sludge. Generally speaking, granular sludge with a larger particle size is better able to resist shocking loadings and adverse conditions. Phenol may be trapped on the surfaces of the anammox granular sludge or may be consumed by the DNB on the surfaces of the SAD granular sludge, resulting in reduced impacts on the internal AMX and a long-term

Table 3

Particle size distribution in the hybrid UASB reactor at the inoculation stage and at the end of the operation

Particle size (mm)	0–0.5	0.5–1.0	1.0–1.5	1.5–2.0	2.0–2.5	>2.5
Inoculation stage	19.22	32.3	17.83	16.22	8.22	6.21
End of the operation	4.87	22.28	15.72	30.87	13.87	12.39

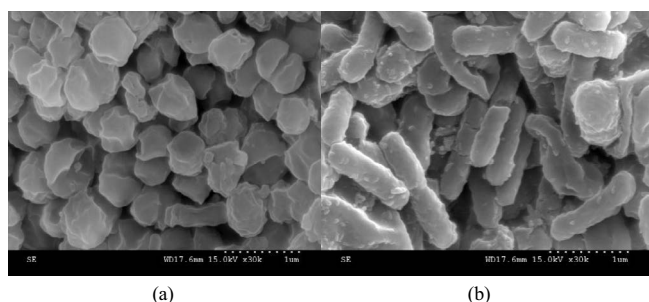


Fig. 7. SEM images of the functional bacteria in the SAD granular sludge ( $\times 30K$ ). (a) AMX and (b) DNB.

stability of the system. The average particle size of the granular sludge increased, and the major fraction changed from the range of 0–1.5 mm (69.4%) at the inoculation stage to the range of 0.5–2.0 mm (68.9%) after domestication with the addition of phenol.

#### 4. Conclusions

The SAD process started up successfully in a hybrid UASB reactor by a stepwise feeding of phenol in the range of 0–18.8 mg L<sup>-1</sup>. A coupled anammox and denitrification process using phenol as the sole carbon source was achieved under low COD/N ratios ( $\leq 0.34$ ). The synergy and competition levels between the AMX and DNB were strongly dependent on the COD/N ratios. The contribution percentage of the nitrogen removal for the anammox route decreased, whereas the denitrification route increased with the increase in the COD/N ratio (0.34–1.18). Moreover, the AMX activity recovered rapidly when the COD/N ratio was decreased back to 0.30. The stable long-term operation of the SAD process was achieved at a COD/N ratio of 0.32, and the average NRR and NLR were 2.53 and 2.26 kg m<sup>-3</sup> d<sup>-1</sup>, respectively. The morphology of the granular sludge indicated that, in addition to the growth of the anammox granular sludge, DNB and SAD granular sludges were formed after domestication with the phenol addition, resulting in an increased average particle size of the granular sludges. Nevertheless, further studies are still required to determine the dominant species of the functional microorganisms (AMX and DNB) by molecular biomethods.

#### Acknowledgements

This work was financially supported by the Hebei Provincial Natural Science Fund Project (E2016402017) and the Handan Science and Technology Research & Development Plan (1623209044).

#### References

- [1] B. Ma, W. Qian, C.S. Yuan, Z.G. Yuan, Y.Z. Peng, Achieving mainstream nitrogen removal through coupling anammox with denitrification, *Environ. Sci. Technol.*, 51 (2017) 8405–8413.
- [2] J.L. Li, L. Zhang, Y.Z. Peng, Q. Zhang, Effect of low COD/N ratios on stability of single-stage partial nitrification/anammox (SPN/A) process in a long-term operation, *Bioresour. Technol.*, 244 (2017) 192–197.
- [3] X. Zhou, X.Z. Wang, H. Zhang, H.M. Wu, Enhanced nitrogen removal of low C/N domestic wastewater using a biochar-amended aerated vertical flow constructed wetland, *Bioresour. Technol.*, 241 (2017) 269–275.
- [4] L.M. Wang, X. Wang, F. Yang, M. Kong, F.Q. Peng, J.Y. Chao, Y.X. Gao, D. Wu, Y.M. Zhu, Y.M. Zhang, Nitrogen removal performance and ammonia- and nitrite-oxidizing bacterial community analysis of a novel industrial waste-based biofilter, *Chem. Eng. J.*, 299 (2016) 156–166.
- [5] X.B. Zhang, Z. Song, W.S. Guo, Y.M. Lu, L. Qi, H.T. Wen, H.H. Ngo, Behavior of nitrogen removal in an aerobic sponge based moving bed biofilm reactor, *Bioresour. Technol.*, 245 (2017) 1282–1285.
- [6] D.W. Gao, Y. Tao, Versatility and application of anaerobic ammonium-oxidizing bacteria, *Appl. Microbiol. Biotechnol.*, 91 (2011) 887–894.
- [7] E. Marañón, I. Vázquez, J. Rodríguez, L. Castrillón, Y. Fernández, Coke wastewater treatment by a three-step activated sludge system, *Water Air Soil Pollut.*, 192 (2008) 155–164.
- [8] L. Amor, M. Eiroa, C. Kennes, M.C. Veiga, Phenol biodegradation and its effect on the nitrification process, *Water Res.*, 39 (2005) 2915–2920.
- [9] G.F. Yang, R.C. Jin, The joint inhibitory effects of phenol, copper (II), oxytetracycline (OTC) and sulfide on Anammox activity, *Bioresour. Technol.*, 126 (2012) 187–192.
- [10] R. Du, Y.Z. Peng, S.B. Cao, C.C. Wu, D.C. Weng, S.Y. Wang, J.Z. He, Advanced nitrogen removal with simultaneous anammox and denitrification in sequencing batch reactor, *Bioresour. Technol.*, 162 (2014) 316–322.
- [11] M. Takekawa, G. Park, S. Soda, M. Ike, Simultaneous anammox and denitrification (SAD) process in sequencing batch reactors, *Bioresour. Technol.*, 174 (2014) 159–166.
- [12] S. Qiao, X. Yin, J.T. Zhou, L.E. Wei, J.Y. Zhong, Integrating anammox with the autotrophic denitrification process via electrochemistry technology, *Chemosphere*, 195 (2018) 817–824.
- [13] C.H. Ge, N. Sun, Q. Kang, L.F. Ren, H.A. Ahmad, S.Q. Ni, Z.B. Wang, Bacterial community evolutions driven by organic matter and powder activated carbon in simultaneous anammox and denitrification (SAD) process, *Bioresour. Technol.*, 251 (2018) 13–21.
- [14] E.A. Giustinianovich, J.L. Campos, M.D. Roedel, The presence of organic matter during autotrophic nitrogen removal: Problem or opportunity? *Sep. Purif. Technol.*, 166 (2016) 102–108.
- [15] F.J. Cervantes, D.A. De la Rosa, J. Gómez, Nitrogen removal from wastewaters at low C/N ratios with ammonium and acetate as electron donors, *Bioresour. Technol.*, 79 (2001) 165–170.
- [16] S.L. He, W. Yang, M. Qin, Z. Mao, Q.G. Niu, M. Han, Performance and microbial community of anammox in presence of micro-molecule carbon source, *Chemosphere*, 205 (2018) 545–552.
- [17] Y.J. Qin, Y. Cao, J.Y. Ren, T.Y. Wang, B. Han, Effect of glucose on nitrogen removal and microbial community in anammox-denitrification system, *Bioresour. Technol.*, 244 (2017) 33–39.
- [18] S.X. Sheng, B. Liu, X.Y. Hou, Z. Liang, X.B. Sun, L.F. Du, D.P. Wang, Effects of different carbon sources and C/N ratios on the simultaneous anammox and denitrification process, *Int. Biodeterior. Biodegrad.*, 127 (2018) 26–34.
- [19] F. Cervantes, O. Monroy, J. Gómez, Influence of ammonium on the performance of a denitrifying culture under heterotrophic conditions, *Appl. Biochem. Biotechnol.*, 81 (1999) 13–21.
- [20] J. Li, Z.M. Qiang, D.S. Yu, D. Wang, P.Y. Zhang, Y. Li, Performance and microbial community of simultaneous anammox and denitrification (SAD) process in a sequencing batch reactor, *Bioresour. Technol.*, 218 (2016) 1064–1072.
- [21] R.C. Jin, Q.Q. Zhang, G.F. Yang, B.S. Xing, Y.X. Ji, H. Chen, Evaluating the recovery performance of the ANAMMOX process following inhibition by phenol and sulfide, *Bioresour. Technol.*, 142 (2013) 162–170.
- [22] C. Ramos, M.E. Suárez-Ojeda, J. Carrera, Denitrification in an anoxic granular reactor using phenol as sole organic carbon source, *Chem. Eng. J.*, 288 (2016) 289–297.
- [23] G. González-Blanco, F. Cuervo-López, F.J. Cervantes, R. Beristain-Cardoso, J. Gomez, Nitrite as oxidizing power for

- p-cresol removal using a denitrifying sludge: kinetic study, *J. Chem. Technol. Biotechnol.*, 88 (2013) 2176–2180.
- [24] G. González-Blanco, R. Beristain-Cardoso, F. Cuervo-López, F.J. Cervantes, J. Gómez, Simultaneous oxidation of ammonium and p-cresol linked to nitrite reduction by denitrifying sludge, *Bioresour. Technol.*, 103 (2012) 48–55.
- [25] APHA-American Public Health Association, *Standard Methods for Water and sewage Examination*, 21st ed., American Public Health Association, Washington, DC, USA, 2005.
- [26] A.D. Pereira, C.D. Leal, M.F. Dias, C. Etchebehere, C.A.L. Chernicharo, J.C.D. Araújo, Effect of phenol on the nitrogen removal performance and microbial community structure and composition of an anammox reactor, *Bioresour. Technol.*, 166 (2014) 103–111.
- [27] M. Strous, J.J. Heijnen, J.G. Kuenen, M.S.M. Jetten, The sequencing batch reactor as a powerful tool for the study of slowly growing anaerobic ammonium-oxidizing microorganisms, *Appl. Microbiol. Biotechnol.*, 50 (1998) 589–596.
- [28] R. Beristain-Cardoso, A.-C. Texier, Á. Alpuche-Solis, J. Gómez, E. Razo-Flores, Phenol and sulfide oxidation in a denitrifying biofilm reactor and its microbial community analysis, *Process Biochem.*, 41 (2009) 23–28.
- [29] C.J. Tang, P. Zheng, C.H. Wang, Q. Mahmood, Suppression of anaerobic ammonium oxidizers under high organic content in high-rate anammox UASB reactor, *Bioresour. Technol.*, 101 (2010) 1762–1768.
- [30] L.V. Niftrik, W.J.C. Geerts, E.G.V. Donselaar, B.M. Humbel, R.I. Webb, J.A. Fuerst, A.J. Verkleij, M.S.M. Jetten, M. Strous, Linking ultrastructure and function in four genera of anaerobic ammonium-oxidizing bacteria: cell plan, glycogen storage, and localization of cytochrome *c* proteins, *J. Bacteriol.*, 190 (2008) 708–711.